

Structural Dependence of NH Stretch Mode Frequency Shifts in Amide and Peptide Systems

Noemi G. Mirkin and Samuel Krimm*

Biophysics Research Division and Department of Physics, University of Michigan, Ann Arbor, Michigan 48109

Received: January 22, 2004; In Final Form: March 31, 2004

The NH stretch (ν) frequency, $\nu(\text{NH})$, in peptides and proteins, as in many amide group hydrogen bond (HB) systems, is used as an indicator of the presence and strength of the bond. This is based on the concept that $\nu(\text{NH})$ is associated with an essentially localized mode whose frequency is influenced only by the HB interaction. We examine this assumption through ab initio studies of *N*-methylacetamide (NMA) and of 78 conformers of the alanine dipeptide (ADP). Based on our recent studies of nitrogen pyramidalization in NMA (*J. Phys. Chem. A* 2003, 107, 1825), we find that such nonplanarity, whether deriving from a nonplanar peptide group or only from a steric constraint, results in an increase in the NH bond length, $r(\text{NH})$, and thus in a decrease in $\nu(\text{NH})$. This is accompanied by changes in other internal coordinates that make small contributions to this mode, emphasizing that although NH ν is a highly localized mode it is not completely so. It is not surprising, therefore, to find that changes in the environment of the NH group, such as exist in the ADP conformers, lead to variations in $\nu(\text{NH})$ even in the absence of traditional HB configurations. The ADP results permit an analysis of these effects and also illustrate the important role, as we recently emphasized (*J. Phys. Chem. A* 2002, 106, 11663), of electrical interactions in affecting $r(\text{NH})$ and thus $\nu(\text{NH})$. We show how the increased strength of this interaction in ADP conformers with “standard” HBs leads, through the much larger induced dipole derivative, to the large increase in infrared intensity of NH ν bands in such structures.

1. Introduction

It has long been recognized that hydrogen bonding of donor X–H groups such as O–H and N–H, for example, in OH \cdots O and N–H \cdots O cases, leads to a red-shift of the X–H stretch (ν) frequency, $\nu(\text{XH})$, from that of the free group.¹ The presence of such shifts has been taken as an indication of hydrogen bonding, with the magnitude of the shift being indicative of the strength of this interaction.

The origin of this frequency shift has been made clear by earlier as well as more recent ab initio studies. In the cases of both OH² and NH,³ increased hydrogen bond (HB) strengths (e.g., associated with shorter H \cdots O distances) lead to longer X–H bond lengths, $r(\text{XH})$, and smaller X–H force constants, which results in lower $\nu(\text{XH})$. Further studies have shown that the bond lengthening originates from an elongating force arising from electrostatic⁴ and electric field–dipole derivative^{5,6} (or equivalent charge flux⁷) interactions that, combined with the contracting effect of the exchange repulsion force at the equilibrium HB position,^{5,8,9} give the observed net bond elongation and thus the frequency red-shift.

The earlier ab initio work³ involved a study of vibrational properties of the hydrogen-bonded NH of *N*-methylacetamide (NMA). In these calculations the peptide group (–CONH–) was kept planar, and the (optimized) NH bond properties (length, force constant, dipole derivative) were obtained as a function of the HB geometry in an NMA–formamide dimer. The assumption of peptide group planarity, that is, $\omega = 0^\circ$, is an undesirable constraint, potentially hiding other factors affecting

the NH group, and recent work¹⁰ has indeed revealed that peptide nonplanarity produces changes in the NH out-of-plane bend (ob) coordinate, γ , which might well lead to changes in $r(\text{NH})$. This will not only have an impact on the spectroscopic properties, which are important in vibrational analyses of peptides and proteins, but associated changes in charge distribution could also have important implications for the representation of peptide groups in molecular mechanics energy functions.^{10,11}

We recently calculated a vibrational frequency map for the alanine dipeptide (ADP), CH₃CONHC ^{α} H(CH₃)CONHCH₃, that is, frequency as a function of dihedral angles φ , CNC ^{α} C, and ψ , NC ^{α} CN, and presented results for the amide III mode.¹² We now present results for the NH ν mode and describe the dependence of its frequency on nitrogen pyramidalization, local electric field effects, hydrogen bonding, and other influences. We preface the discussion of the ADP with an examination of the relevant parameters in the simpler case of the amide group of NMA.

2. Calculations

All ab initio molecular orbital calculations were performed with the Gaussian 98¹³ program.

In the first set of calculations for NMA and NMA–H₂O, performed with density functional theory (DFT), the B3LYP functional, and the 6-31+G* basis set (which we showed gives a planar peptide group at equilibrium¹⁴), we studied geometries and frequencies as a function of γ for various deformations of the peptide CN torsion angle, ω . For the ω coordinate we use the nonredundant Bell’s torsion,¹⁵ defined as the average of the OCNC and CCNH dihedral angles. This coordinate measures the angle between the π -orbitals of the peptide group and is

* Corresponding author. Phone: 734-763-8081. Fax: 734-764-3323. E-mail: skrimm@umich.edu.

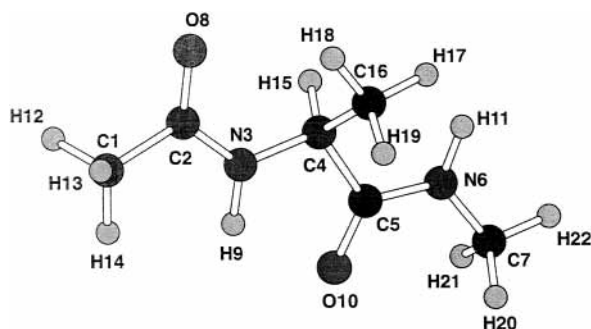


Figure 1. Alanine dipeptide in the $\varphi(\text{C}_2\text{N}_3\text{C}_4\text{C}_5) = -180^\circ$, $\psi(\text{N}_3\text{C}_4\text{C}_5\text{N}_6) = 180^\circ$ conformation.

orthogonal to γ .¹¹ These angles were set to values that yielded the desired range of γ (-35.6° to 35.6°) and ω (0° to 20°).

In the second set of calculations involving NMA, performed at MP2/6-31++G**, we looked at the changes in geometry, and in particular γ and ω , as we increased and fixed $r(\text{NH})$ by 0.5, 1.5, and 2.0% of the equilibrium value and fully optimized the rest of the geometry parameters. We did the same for $r(\text{CO})$, increasing it by 2% of the equilibrium value. Moreover, given that an increase of $r(\text{NH})$ causes a rotation of the methyl (Me) groups (i.e., 8.3° for the CMe and 9.0° for the NMe, for $\Delta r(\text{NH}) = 1.5\%$), we also fixed the torsion angles $\tau(\text{CMe})$ and $\tau(\text{NMe})$ separately (fully optimizing everything else) to study the effects on $r(\text{NH})$, γ , and ω .

In our previous work on the ADP,¹² the molecule being shown in Figure 1, we studied 48 conformers that span the mostly low-energy φ , ψ region of the isolated molecule map. The ADP geometry optimizations and frequency calculations were performed at the B3LYP/6-31+G* level. In the present work we have added more conformations and now have a total of 78 conformers. At each value of φ , ψ all the other geometry parameters were fully optimized and the frequencies and normal modes were calculated.

In a recent paper, Schweitzer-Stenner et al.¹⁶ described this approach as “problematic from a physical point of view” due to the existence of nonvanishing forces associated with the constrained angles. Since all the forces are zero except for those related to the fixed φ and ψ dihedral angles, this does not necessarily result in uniformly “coordinate-dependent frequencies” as claimed by Schweitzer-Stenner and collaborators: although the constraints on φ and ψ will affect the lower frequencies, in particular those involving φ and ψ torsion, the higher frequencies may not be affected significantly. The effect of the constraints can be evaluated by examining the Jacobian elements (change in frequency with change in force constant), both in absolute value and as a function of conformation. For the six equilibrium ADP structures of different φ , ψ , we find this element to be essentially zero for all $\partial\nu(\text{NH})/\partial f(\varphi)$ and $\partial\nu(\text{NH})/\partial f(\psi)$. Thus, $\nu(\text{NH})$ is not influenced by constraining only φ and ψ and optimizing the structure with respect to all other coordinates, and any changes with conformation must be attributed to other factors.

In order to study the φ , ψ dependence of the amide modes of the ADP, it is important to have vibrational frequencies and eigenvectors that are as experimentally accurate as possible. It is therefore desirable to have scaled vibrational frequencies. Scale factors were obtained by scaling the force constants of the lowest energy equilibrium conformer, C7eq, to reproduce carefully assigned observed frequencies of the matrix isolated species.¹⁷ Based on the excellent reproduction of the experimental frequencies of the C7eq and C5 conformers and their

TABLE 1: Bond Lengths and NH Stretch Frequencies of N-Methylacetamide as a Function of Peptide Torsion (ω) and NH Out-of-Plane Bend (γ) Angles^a

ω^b	γ^b	$r(\text{NH})^c$	$r(\text{CN})^c$	$r(\text{CO})^c$	ν^d
0	0.0	1.0094	1.3652	1.2291	3500
	8.7	1.0096	1.3662	1.2288	3496
	17.5	1.0104	1.3687	1.2283	3484
	26.4	1.0115	1.3724	1.2276	3469
	35.6	1.0127	1.3769	1.2266	3452
10	-35.6	1.0133	1.3801	1.2259	3442
	-26.4	1.0120	1.3757	1.2268	3460
	-17.5	1.0111	1.3725	1.2275	3474
	-8.7	1.0105	1.3707	1.2279	3483
	0.0	1.0095	1.3668	1.2287	3497
15	8.7	1.0098	1.3675	1.2286	3493
	17.5	1.0104	1.3695	1.2282	3485
	26.4	1.0113	1.3725	1.2276	3474
	35.6	1.0125	1.3767	1.2268	3458
	20	0.0	1.0100	1.3693	1.2281
8.7		1.0100	1.3692	1.2282	3492
17.5		1.0105	1.3710	1.2278	3485
26.4		1.0114	1.3739	1.2273	3475
35.6		1.0126	1.3780	1.2265	3458
20	0.0	1.0104	1.3726	1.2274	3484
	8.7	1.0101	1.3713	1.2277	3490
	17.5	1.0106	1.3729	1.2275	3485
	26.4	1.0115	1.3759	1.2269	3472
	35.6	1.0129	1.3799	1.2264	3456

^a NH stretch frequencies from B3LYP/6-31+G* calculations. ^b In degrees. ^c In angstroms. ^d Scaled, in cm^{-1} .

deuterated species,¹⁸ we thus had a reliable set of scale factors that was then used to scale the frequencies of all the φ , ψ conformers.

3. Results and Discussion

3.1. N-Methylacetamide. Our previous studies¹⁰ have shown that departures from peptide group planarity, that is, nonzero values of ω , lead to equilibrium departures from planarity at the N atom, that is, to nonzero values of γ , corresponding to pyramidalization at this atom. We now examine the specific geometric and spectroscopic changes associated with these departures, as they affect $\nu(\text{NH})$, in the simple case of the single peptide group of NMA, first for the isolated molecule and then in the case of hydrogen bonding to the NH group. (Examination of the appropriate Jacobian elements again shows that changes in $\nu(\text{NH})$ are essentially independent of constraints on ω and γ .)

3.1.1. Isolated NMA. In the first set of calculations (B3LYP/6-31+G*), constraints were imposed on ω and γ , with some resulting geometries and the corresponding $\nu(\text{NH})$ being given in Table 1. It is clear from these results that the NH bond lengthens with increasing $|\gamma|$ (Figure 2), almost independent of ω (for $\omega = 0^\circ$ and $\gamma = 35.6^\circ$, $\Delta r(\text{NH}) = 0.33\%$; for $\omega = 20^\circ$ and $\gamma = 35.6^\circ$, $\Delta r(\text{NH}) = 0.25\%$). Associated with this bond elongation, the NH s frequency therefore decreases: for $|\Delta\gamma| \cong 35^\circ$ the red-shift is of the order of 30–50 cm^{-1} . The $r(\text{NH})$ dependence on the sign of γ is slightly asymmetric (cf. the case for $\omega = 10^\circ$) since asymmetry is introduced in the peptide group by the sign of ω . The dependence of $r(\text{NH})$ on $|\gamma|$ is slightly nonlinear, probably because the equilibrium value of γ , that is, γ_0 , varies with ω . For example, while $\gamma_0 = 0^\circ$ for $\omega = 0^\circ$, $\gamma_0 = 20^\circ$ for $\omega = 10^\circ$.¹⁰ It is also seen that $r(\text{CN})$ increases and $r(\text{CO})$ decreases with increasing $|\gamma|$. It is worth noting that, whereas the same $r(\text{NH})$ can occur for different sets of ω and γ , for example, $\omega = 0^\circ$, $\gamma = 17.5^\circ$; $\omega = 10^\circ$, $\gamma = 17.5^\circ$; and $\omega = 20^\circ$, $\gamma = 0^\circ$, and therefore can exhibit the same $\nu(\text{NH})$,

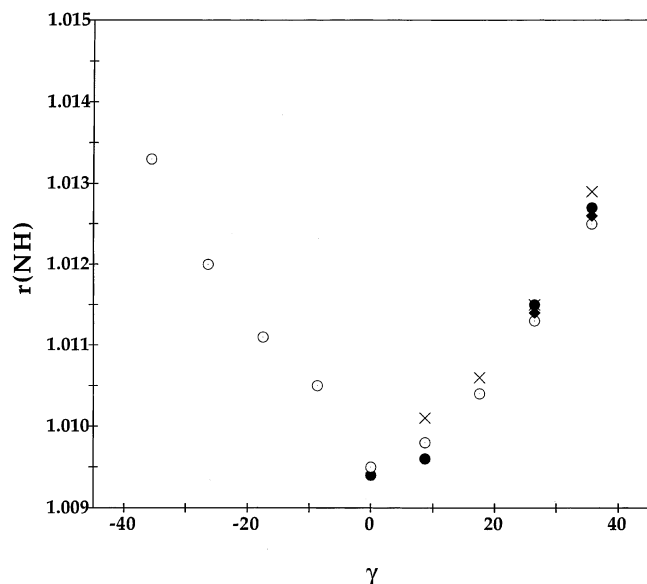


Figure 2. NH bond length (in angstroms) of *N*-methylacetamide as a function of the nitrogen pyramidalization angle γ (in degrees) for different values of the (Bell) peptide torsion angle ω : \bullet , 0° ; \circ , 10° ; \blacklozenge , 15° ; \times , 20° .

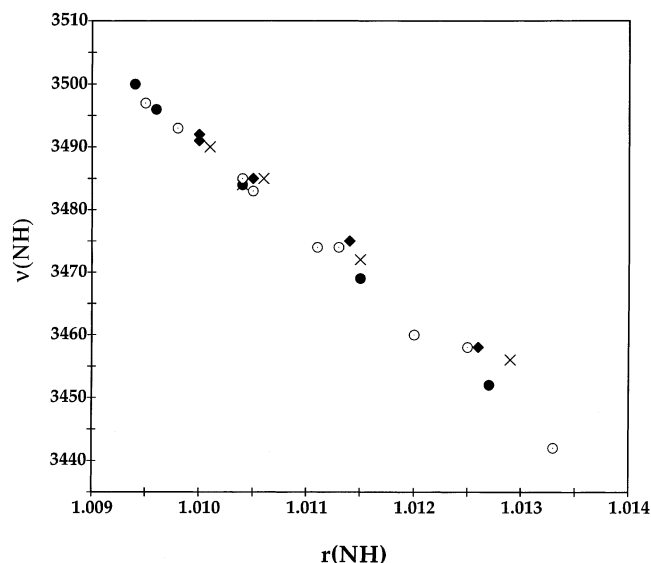


Figure 3. NH stretch frequency (in cm^{-1}) of *N*-methylacetamide as a function of the NH bond length (in angstroms) for various values of the peptide torsion angle ω : \bullet , 0° ; \circ , 10° ; \blacklozenge , 15° ; \times , 20° .

their $r(\text{CN})$ and $r(\text{CO})$ can be quite different. Thus, the NH s frequency is not necessarily a guide to the overall geometry of the peptide group.

The dependence of $\nu(\text{NH})$ on $r(\text{NH})$ is shown in Figure 3 and is seen to be, with very little variation, linear over this range with a very small dependence on ω . It is worth noting that this linearity does not imply a constancy of the NH s eigenvector with $r(\text{NH})$. Although this mode is usually thought of as being completely localized, in fact it contains nontrivial contributions from other coordinates, some of which change significantly with γ . This is shown in Table 2 for $\omega = 0^\circ$ and a plot of the variation with γ of the NH ob component of the NH s mode eigenvector for various ω is shown in Figure 4. In this case (as for CN torsion (t) and NC(Me) t) the eigenvector contribution is proportional to $|\gamma|$. This arises from the near proportionality between the cross-term force constant $f(\text{NH s}, \text{NH ob})$ and $|\gamma|$. For $\omega = 0^\circ$, this force constant is zero at $\gamma = 0^\circ$, by planar symmetry, and decreases (to -0.149 for $\gamma = 35.6^\circ$) apparently

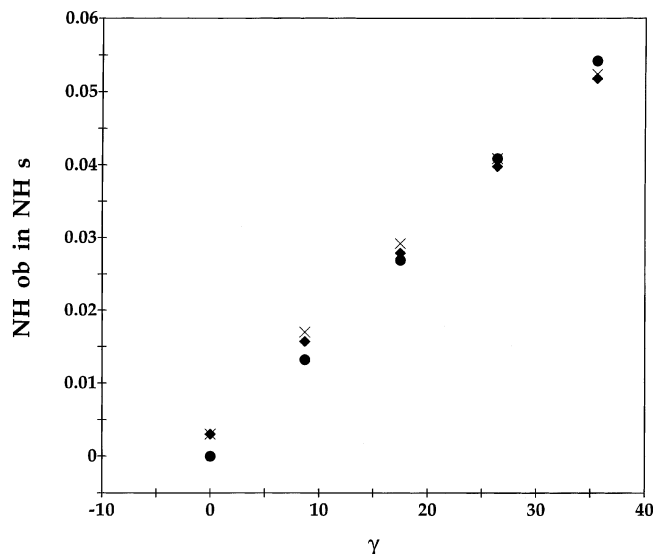


Figure 4. NH out-of-plane bend coordinate component of the NH stretch eigenvector of *N*-methylacetamide (NH stretch coordinate component = 1.000) as a function of the nitrogen pyramidalization angle γ (in degrees) for various values of the peptide torsion angle ω : \bullet , 0° ; \blacklozenge , 15° ; \times , 20° .

TABLE 2: Eigenvector Components of the NH Stretch Mode of Planar *N*-Methylacetamide as a Function of the NH Out-of-Plane Bend (γ) Angle^{a,b}

coordinate ^d	γ^c				
	0	8.7	17.5	26.4	35.6
NH s	1.000	1.000	1.000	1.000	1.000
CN s	-0.036	-0.035	-0.035	-0.033	-0.032
NC(Me) s ^e	-0.035	-0.034	-0.033	-0.032	-0.030
C(Me)CN d ^e	0.053	0.053	0.053	0.052	0.051
CNC(Me) d ^e	0.102	0.102	0.099	0.095	0.090
CO ib	0.027	0.027	0.027	0.027	0.027
NH ib	0.001	0.001	0.000	0.001	0.001
(N)CH ₃ r1	-0.052	0.051	-0.047	-0.043	-0.040
(N)CH ₃ r2	0.000	0.012	0.022	0.030	0.034
NH ob	0.000	-0.018	-0.026	-0.040	-0.053
CN t	0.000	-0.008	-0.015	-0.021	-0.027
NC(Me) t ^e	0.000	0.008	0.016	0.023	0.029

^a For the eigenvector components, the sign indicates the relative phase of the coordinate. ^b Planar *N*-methylacetamide, $\omega = 0^\circ$. ^c In degrees. ^d s = stretch, d = deformation, ib = in-plane bend,²³ r1 = in-plane rock,²³ r2 = out-of-plane rock,²³ ob = out-of-plane bend, t = torsion. ^e Me = methyl group.

due to the increase in the environmental asymmetry of the NH group with the increase in $|\gamma|$. For $\omega \neq 0^\circ$ but $\gamma = 0^\circ$, $f(\text{NH s}, \text{NH ob}) \neq 0$, consistent with this explanation.

In another set of calculations (MP2/6-31++G**), the effects on the geometry of other single constraints were examined (Table 3). It is seen that even small changes in $r(\text{NH})$, which might result from the elongating force of a local electric field,⁶ cause significant changes in the geometry of the rest of the peptide group. On the other hand, changes in $r(\text{CO})$ influence $r(\text{CN})$ but have essentially no effect on the other parameters. Interestingly, isolated rotations of the end methyl groups that correspond to a given $r(\text{NH})$, for example, the $\tau(\text{CMe}) = 8.3^\circ$ for $\Delta r(\text{NH}) = 1.5\%$, have only a small effect on $r(\text{NH})$ but produce comparable changes in $r(\text{CN})$, ω , and γ . The differences in the (CHELPG¹⁹) charges in these cases show that the electronic structures are not the same for these different kinds of constraints, which should not be surprising. The molecular dipole derivative with respect to the NH bond, $\partial\mu/\partial r(\text{NH})$, changes relatively little with $\Delta r(\text{NH})$, if anything decreasing slightly. We will have further comments on this below.

TABLE 3: Geometric Parameters, Atomic Charges, and Dipole Derivatives of *N*-Methylacetamide as a Function of NH and CO Bond and Methyl Group Torsion Constraints^a

coordinate	$\Delta r(\text{NH})$				$\Delta r(\text{CO})$	$\tau(\text{CMe})^b$	$\tau(\text{NMe})^c$
	0%	0.5%	1.5%	2.0%	1.0%	8.3°	170.9°
$r(\text{NH})$	1.0061	1.0111	1.0212	1.0262	1.0062	1.0067	1.0066
$r(\text{CN})$	1.3639	1.3657	1.3661	1.3663	1.3618	1.3656	1.3656
$r(\text{CO})$	1.2379	1.2376	1.2376	1.2376	1.2503	1.2376	1.2376
ω^d	0.0	1.6	1.7	1.7	0.0	1.4	1.5
γ^e	0.1	11.1	12.2	12.8	0.1	10.6	10.6
$\tau(\text{CMe})^b$	0.0	7.0	8.3	8.9	0.0	8.3	6.4
$\tau(\text{NMe})^c$	179.9	171.3	170.9	170.7	179.9	171.6	170.9
CHELPG Charges ^f							
$q(\text{N})$	-0.578	-0.619	-0.625	-0.631	-0.591	-0.618	-0.618
$q(\text{H})$	0.320	0.331	0.332	0.332	0.326	0.332	0.331
$q(\text{C})$	0.757	0.787	0.794	0.798	0.760	0.788	0.788
$q(\text{O})$	-0.585	-0.592	-0.593	-0.593	-0.589	-0.592	-0.591
$q(\text{C})(\text{NMe})$	0.014	0.068	0.073	0.086	0.043	0.064	0.066
$q(\text{H})$	0.060	0.046	0.044	0.042	0.051	0.046	0.046
$q(\text{H})$	0.062	0.059	0.058	0.055	0.063	0.059	0.059
$q(\text{H})$	0.061	0.042	0.040	0.036	0.050	0.043	0.042
$q(\text{C})(\text{CMe})$	-0.498	-0.522	-0.533	-0.535	-0.508	-0.528	-0.530
$q(\text{H})$	0.139	0.144	0.146	0.146	0.142	0.145	0.146
$q(\text{H})$	0.109	0.113	0.115	0.116	0.111	0.114	0.115
$q(\text{H})$	0.139	0.145	0.148	0.148	0.143	0.146	0.146
Dipole Derivative ^g							
$\partial\mu/\partial r(\text{NH})$	0.165	0.156	0.152	0.149			

^a MP2/6-31++G** calculations. ^b $\tau(\text{CMe})=\text{HCCN}$, in degrees. ^c $\tau(\text{NMe})=\text{HCNC}$, in degrees. ^d ω = Bell's torsion angle (see text), in degrees. ^e γ = out-of-plane bend angle, in degrees. ^f In electrons. ^g In electrons.

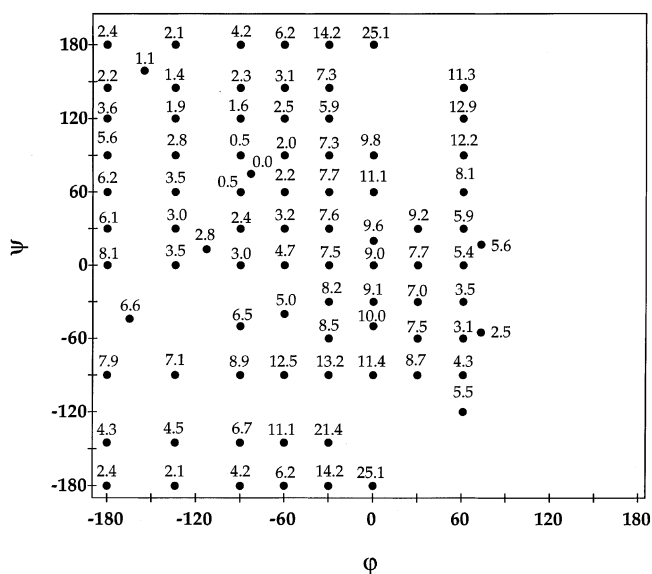
TABLE 4: Bond Lengths and NH Stretch Frequencies of *N*-Methylacetamide-H₂O as a Function of Peptide Torsion (ω) and NH Out-of-Plane Bend (γ) Angles^a

ω^b	γ^b	$r(\text{NH})^c$	$r(\text{CN})^c$	$r(\text{CO})^c$	ν^d
0	0.0	1.0142	1.3610	1.2321	3435
	8.7	1.0145	1.3616	1.2321	3432
	17.5	1.0149	1.3637	1.2316	3426
	26.4	1.0156	1.3671	1.2308	3418
	35.6	1.0165	1.3713	1.2300	3406
15	0.0	1.0144	1.3636	1.2315	3433
	8.7	1.0147	1.3641	1.2315	3429
	17.5	1.0153	1.3658	1.2311	3421
	26.4	1.0160	1.3689	1.2304	3413
	35.6	1.0171	1.3727	1.2298	3399

^a B3LYP/6-31+G* calculations. ^b In degrees. ^c In angstroms. ^d Scaled, in cm^{-1} .

3.1.2. Hydrogen-Bonded NMA. In the case of a hydrogen-bonded (to water) NH group, Table 4, although the variations of $r(\text{NH})$ with $|\gamma|$ are roughly the same as for the nonbonded group, there is a small inverse dependence on ω : for $\omega = 0^\circ$, $\gamma = 35.6^\circ$, $\Delta r(\text{NH}) = 0.33\%$ for NMA and 0.23% for NMA-H₂O, whereas for $\omega = 15^\circ$, $\gamma = 35.6^\circ$, $\Delta r(\text{NH}) = 0.26\%$ for NMA and 0.27% for NMA-H₂O. The frequency shifts with γ and variations with ω are also different: for NMA, the shift from $\gamma = 0^\circ$ to $\gamma = 35.6^\circ$ is 48 cm^{-1} (1.4%) for $\omega = 0^\circ$ and 33 cm^{-1} (1%) for $\omega = 15^\circ$, whereas for NMA-H₂O the comparable shifts are 29 cm^{-1} (0.8%) and 40 cm^{-1} (1.2%). This emphasizes the complex nature of the dependence of $\nu(\text{NH})$ on peptide group geometry and environmental factors such as those involved in HB interactions.

3.2. Alanine Dipeptide. **3.2.1. Overall Energies, Geometries, and Frequencies.** We present in Figure 5 (and in the Supporting Information) the relative energies of the conformers as a function of φ and ψ . In Table 5 we list some geometric parameters and $\nu(\text{NH})$ of peptide group 1 ($\text{C}_2\text{O}_8\text{-N}_3\text{H}_9$) for each conformer, with a vibrational frequency map in Figure 6. Similar results are given for peptide group 2 ($\text{C}_5\text{O}_{10}\text{-N}_6\text{H}_{11}$) in Table 6 and Figure 7.

**Figure 5.** Relative energy map, in kcal/mol, of conformers of the alanine dipeptide as a function of $\varphi(\text{CNC}^{\text{C}})$ and $\psi(\text{NC}^{\text{C}}\text{CN})$ (in degrees).

A glance at these data immediately shows that $r(\text{NH})$, and thus $\nu(\text{NH})$, varies significantly with φ and ψ . The interesting question is whether, from this wealth of data and in view of the composite nature of an ab initio result, we can infer the role of obvious physical factors that determine $r(\text{NH})$ and $\nu(\text{NH})$. In this context we should at least consider the following. (1) Since NH1 (N_3H_9) and NH2 (N_6H_{11}) are in different local chemical environments, it is possible that their behavior may be somewhat different. This suggests examining NH1 and NH2 separately. (2) Based on the NMA results, we can expect that $r(\text{NH})$ will depend on γ , that is, the extent of pyramidalization, but it will also be influenced by other factors, such as nonbonded (van der Waals and electrostatic) interactions and neighboring (non-HB-involved) electric fields.^{6,9} (3) The dependence of $\nu(\text{NH})$ solely on $r(\text{NH})$ is based on the nature of the NH s eigenvector: if internal coordinates other than those associated

TABLE 5: Geometric Parameters and NH Stretch Frequencies in Peptide Group 1 as a Function of φ , ψ Angles in Conformers of the Alanine Dipeptide

φ, ψ^a	ω^b	γ^c	$r(\text{NH})^d$	$r(\text{CN})^d$	$r(\text{CO})^d$	$\nu(\text{NH})^e$	$\text{H}_9 \cdots \text{O}_{10}^d$
-180, 180	2.4	-3.3	1.0154	1.3619	1.2321	3406	2.09
145	-0.3	-19.4	1.0152	1.3665	1.2307	3410	2.24
120	-0.4	-26.2	1.0148	1.3720	1.2288	3416	2.45
90	1.0	-28.2	1.0144	1.3762	1.2271	3418	2.85
60	2.0	-27.5	1.0140	1.3779	1.2260	3419	5.31
30	1.6	-33.4	1.0152	1.3828	1.2246	3401	3.63
0	0.4	-40.0	1.0167	1.3883	1.2234	3377	3.82
-90	4.0	16.0	1.0120	1.3710	1.2280	3449	2.86
-145	5.2	13.1	1.0145	1.3651	1.2310	3419	2.17
-165, -44 (α')	3.1	22.1	1.0123	1.3749	1.2266	3442	3.55
-155, 159 (C5)	0.8	5.4	1.0144	1.3625	1.2319	3423	2.21
-134, 180	3.5	27.0	1.0159	1.3708	1.2301	3400	2.17
145	-1.3	11.6	1.0138	1.3659	1.2310	3434	2.35
120	0.6	0.0	1.0127	1.3666	1.2306	3448	2.61
90	1.1	-11.7	1.0127	1.3699	1.2296	3444	3.04
60	1.7	-15.8	1.0130	1.3729	1.2284	3437	3.51
30	0.6	-20.0	1.0134	1.3775	1.2264	3430	3.86
0	-1.2	-27.4	1.0145	1.3829	1.2245	3414	4.06
-90	-1.6	9.4	1.0114	1.3718	1.2271	3455	3.30
-145	2.9	31.6	1.0141	1.3757	1.2282	3422	2.35
-113, 13 (β_2)	0.9	-16.6	1.0129	1.3769	1.2263	3436	4.09
-90, 180	0.6	31.6	1.0140	1.3796	1.2271	3426	2.59
145	2.9	26.5	1.0136	1.3744	1.2291	3435	2.64
120	3.6	17.8	1.0126	1.3699	1.2308	3448	2.89
90	4.2	2.7	1.0117	1.3639	1.2344	3457	3.35
60	5.2	-6.7	1.0120	1.3608	1.2362	3451	3.78
30	6.7	-9.6	1.0120	1.3634	1.2336	3448	4.07
0	2.0	-11.1	1.0121	1.3742	1.2269	3447	4.26
-50	-1.1	-20.2	1.0128	1.3786	1.2239	3431	4.33
-90	-3.8	22.4	1.0134	1.3820	1.2229	3427	3.61
-145	-3.2	30.8	1.0140	1.3834	1.2246	3419	2.88
-83, 75 (C7eq)	3.8	-0.1	1.0119	1.3613	1.2362	3452	3.59
-60, 180	-3.6	36.8	1.0150	1.3868	1.2244	3406	2.92
145	1.6	29.6	1.0134	1.3758	1.2283	3432	2.98
120	1.7	24.4	1.0129	1.3707	1.2307	3439	3.17
90	-0.8	21.6	1.0133	1.3668	1.2339	3431	3.48
60	-0.7	15.9	1.0130	1.3622	1.2362	3433	3.86
30	2.3	8.0	1.0122	1.3599	1.2365	3444	4.16
0	4.8	0.8	1.0116	1.3635	1.2328	3453	4.33
-40 (α_R)	0.4	-10.5	1.0120	1.3732	1.2258	3447	2.95
-90	-3.9	22.7	1.0135	1.3824	1.2208	3420	4.01
-145	-12.0	40.4	1.0169	1.3980	1.2204	3376	3.15
-30, 180	-16.7	42.2	1.0159	1.3993	1.2204	3384	3.29
145	-6.8	33.9	1.0141	1.3820	1.2256	3416	3.33
120	-4.1	26.8	1.0132	1.3736	1.2280	3428	3.51
90	-6.5	25.1	1.0132	1.3703	1.2303	3425	3.78
60	-7.0	20.8	1.0125	1.3656	1.2344	3433	4.08
30	-3.3	11.8	1.0116	1.3624	1.2357	3444	4.30
0	1.1	3.4	1.0117	1.3612	1.2354	3443	4.40
-30	2.3	1.6	1.0119	1.3647	1.2317	3444	4.45
-60	1.0	-3.2	1.0119	1.3707	1.2267	3445	4.41
-90	7.3	-22.5	1.0133	1.3773	1.2234	3423	4.23
-145	-22.3	42.7	1.0167	1.4066	1.2155	3368	3.61
0, 180	-23.2	34.9	1.0134	1.4009	1.2154	3408	3.78
90	-4.1	13.9	1.0122	1.3710	1.2270	3440	4.12
60	-3.8	5.7	1.0119	1.3656	1.2309	3443	4.36
20	-1.9	3.2	1.0120	1.3614	1.2355	3437	4.43
0	0.6	-0.2	1.0123	1.3609	1.2359	3435	4.42
-30	4.0	-5.2	1.0125	1.3614	1.2351	3433	4.40
-50	5.5	-8.5	1.0125	1.3632	1.2332	3434	4.36
-90	4.4	-14.3	1.0123	1.3711	1.2270	3439	4.10
30, 30	-2.6	3.3	1.0116	1.3634	1.2326	3448	4.46
0	-0.9	-0.4	1.0117	1.3602	1.2359	3445	4.40
-30	2.6	-7.9	1.0116	1.3609	1.2361	3446	4.29
-60	6.0	-16.7	1.0117	1.3639	1.2346	3446	4.11
-90	6.1	-22.8	1.0119	1.3696	1.2305	3443	3.79

with pyramidalization, as in NMA, contribute and change as a function of backbone conformation, $\nu(\text{NH})$ could vary from other regular $r(\text{NH})$ relationships. (A similar effect could occur if transition dipole coupling²⁰⁻²² or unusual kinetic coupling were involved between the two NH groups.) (4) Of course,

formation of a HB type of interaction will have a significant effect on $r(\text{NH})$. We pay particular attention to $r(\text{H} \cdots \text{O}) < 2.5$ Å as an indication of such interactions. Although other factors such as anharmonicity and Fermi resonance can influence $\nu(\text{NH})$, we do not consider these in the present analysis.

TABLE 5: (Continued)

φ, ψ^a	ω^b	γ^c	$r(\text{NH})^d$	$r(\text{CN})^d$	$r(\text{CO})^d$	$\nu(\text{NH})^e$	$\text{H}_9 \cdots \text{O}_{10}^d$
61, 145	10.4	-35.7	1.0142	1.3930	1.2209	3410	3.25
120	9.5	-31.8	1.0137	1.3909	1.2198	3417	3.59
90	1.4	-6.3	1.0102	1.3766	1.2222	3463	4.14
60	-1.8	21.2	1.0122	1.3769	1.2244	3440	4.40
30	-1.7	14.0	1.0114	1.3745	1.2264	3453	4.44
0	-5.7	7.1	1.0111	1.3632	1.2335	3460	4.35
-30	-3.6	-2.4	1.0109	1.3604	1.2365	3460	4.17
-60	-1.0	-10.0	1.0111	1.3620	1.2362	3458	3.91
-90	-0.9	-16.1	1.0111	1.3657	1.2338	3460	3.52
-120	-2.7	-21.3	1.0110	1.3698	1.2305	3462	3.14
73, 17 (α_1)	-4.0	16.3	1.0115	1.3754	1.2265	3453	4.40
73, -55 (C7ax)	-4.7	0.6	1.0107	1.3610	1.2365	3465	3.93

^a Torsion angles: $\varphi = \tau(\text{C}_2\text{N}_3\text{C}_4\text{C}_5)$, $\psi = \tau(\text{N}_3\text{C}_4\text{C}_5\text{N}_6)$, in degrees. ^b Peptide group (Bell's) torsion angle, in degrees. ^c NH out-of-plane bend angle, in degrees. The sign of γ is defined as follows: referring to Figure 1, in the planar sequence $\text{C}_2\text{-N}_3\text{H}_9\text{-C}_4$, positive γ corresponds to the displacement of H in the direction of a right-handed screw advancing with a rotation of $\text{H}_9\text{-C}_2\text{-C}_4$. ^d In angstroms. ^e In cm^{-1} .

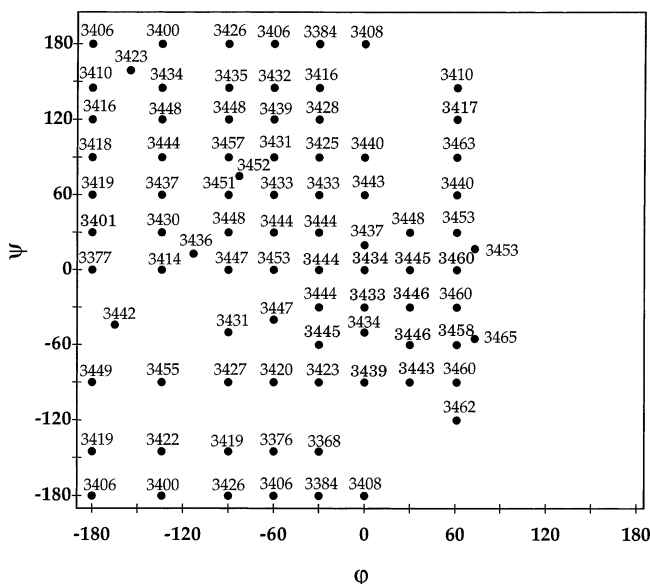


Figure 6. NH1 stretch vibrational frequency map (in cm^{-1}) of conformers of the alanine dipeptide as a function of $\varphi(\text{CNC}^0\text{C})$ and $\psi(\text{NC}^0\text{CN})$ (in degrees).

3.2.2. Peptide Group 1. A striking feature of $\nu(\text{NH}1)$ is that it can vary by almost 100 cm^{-1} among conformations in which group 1 clearly does not participate in any HBs, viz., 3368 cm^{-1} (for $-30, -145$) to 3463 cm^{-1} (for $61, 90$). In fact, none of the most “red-shifted” frequencies, viz., 3368 ($-30, -145$), 3376 ($-60, -145$), 3377 ($-180, 0$), and 3384 ($-30, 180$) cm^{-1} , involve structures with HBs, but they do have large $|\gamma|$ (of the order of 40°) and thus are dominated by the pyramidalization lengthening of $r(\text{NH})$, as in NMA. Examination of these structures reveals that the large $|\gamma|$ is a result of two main effects: in the case of $-180, 0$, H_9 and H_{11} are unacceptably close (2.05 \AA) and, even though $\omega_1 \sim 0^\circ$, $\gamma_1 = -40^\circ$ to relieve the steric and electrostatic repulsions (in the case of NH_2 , a smaller γ , 26.8° , is possible because $\omega_2 = 10^\circ$); in the other cases, O_8 and O_{10} come close ($2.80, 3.51$, and 2.81 \AA , respectively), and the strain is relieved primarily by changes in ω with accompanying changes in γ .¹⁰ However, a general expectation that $r(\text{NH})$ relates only to γ , in the simple way of NMA (cf. Figure 2), is countered by the data, as shown in Figure 8, and it is therefore not surprising that a $\nu(\text{NH})\text{-}r(\text{NH})$ plot, Figure 9, while showing the expected trend, exhibits significantly more variation than the simple plot of NMA (cf. Figure 3). We return below to a discussion of possible reasons for this behavior.

At the “blue-shifted” end of the frequency range ($\geq 3460 \text{ cm}^{-1}$), other factors operate to decrease $r(\text{NH})$ and therefore to

increase $\nu(\text{NH})$. For example, for the $61, 90$ structure (Figure 10) the $\text{H}_9 \cdots \text{H}_{11}$ and $\text{O}_8 \cdots \text{O}_{10}$ distances are long (3.19 and 3.18 \AA respectively) and γ is small, -6.3° , but the dipolar electric field of peptide group 2 at peptide group 1 is such that the field and the $\text{N}_3 \rightarrow \text{H}_9$ dipole derivative are antiparallel. As we,^{6,9} and others,⁵ have shown, this results in a contracting force on this bond, leading to its shortening and thus the increase in its frequency. While this effect had previously been discussed in connection with hydrogen bonding, it is clear that it operates in general⁹ and thus needs to be incorporated in thinking about physical factors that govern structural change.

The same kind of interaction, but in a parallel orientation of the dipolar electric field and dipole derivative, can account for the generally longer $r(\text{NH})$, and therefore lower $\nu(\text{NH})$, $3400\text{--}3434 \text{ cm}^{-1}$, of the eight structures for which $r(\text{H}_9 \cdots \text{O}_{10}) < 2.5 \text{ \AA}$ (which mainly fall in a separate category in the $r\text{-}\gamma$ plot, Figure 8). Although such structures, as exemplified by the $-180, 180$ conformer (Figure 1), have been spoken of in terms of a “hydrogen bond” between N_3H_9 and C_5O_{10} , there are good reasons not to characterize it as such: the nearly parallel bonds contrast with the roughly colinear arrangements in standard HBs, the $\text{H}_9 \cdots \text{O}_{10}$ distances ($2.09\text{--}2.45 \text{ \AA}$) are significantly longer than those of typical HBs (compare these to the $1.72\text{--}1.79 \text{ \AA}$ of the strong HBs of peptide group 2), and the “red-shift” is considerably smaller (we consider below the assignment of an “unperturbed” $\nu(\text{NH}1)$). In fact, in the spirit that such shifts result from the same kinds of forces on X–H bonds which, together with steric repulsion, determine their spectroscopic characteristics,⁹ we should consider all of these “bonds” to partake of the same nature, from blue-shifted CH s in $\text{C}\text{-H} \cdots \text{O}$ groups,⁹ through slightly red-shifted NH s in the ADP’s group 1, to strongly red-shifted NH s in “standard” $\text{N}\text{-H} \cdots \text{O}$ interactions. There is, however, a special consequence of the $\text{NH} \cdots \text{OC}$ interaction in the current case: as found previously,³ the CNH angle increases with decreasing $r(\text{H} \cdots \text{O})$ in such ADP structures, probably mainly as a result of the electrostatic interaction between the positive H_9 and negative O_{10} . As seen in Table 7 for the $\varphi = -180^\circ$ structures, the related symmetry coordinate, the NH in-plane bend²³ (ib) angle, increases by about 7° as the conformation approaches the “hydrogen-bonded” structure, with an increasing $r(\text{NH})$ and an increase in the contribution of NH ib to the NH s eigenvector. This is associated with an increase in $f(\text{NH} \text{ s}, \text{NH ib})$, which is probably a result of the increasingly asymmetric environment in which this motion takes place, it being nearly symmetric in NMA and thus resulting in $f(\text{NH} \text{ s}, \text{NH ib}) \cong 0$. (As in the case of NMA, the NH ob contribution to the NH s mode increases with $|\gamma|$.) The trend of $r(\text{NH})$ with γ is counter to that of NMA and is due to at

TABLE 6: Geometric Parameters and NH Stretch Frequencies in Peptide Group 2 as a Function of φ , ψ Angles in Conformers of the Alanine Dipeptide

φ, ψ^a	ω^b	γ^c	$r(\text{NH})^d$	$r(\text{CN})^d$	$r(\text{CO})^d$	$\nu(\text{NH})^e$	$\text{H}_{11}\cdots\text{O}_8^d$
-180, 180	-0.8	-4.4	1.0100	1.3560	1.2324	3476	5.24
145	-2.4	2.0	1.0104	1.3565	1.2318	3470	5.06
120	-1.4	-1.8	1.0101	1.3571	1.2313	3475	4.89
90	0.4	-3.5	1.0105	1.3597	1.2293	3470	4.62
60	-0.4	1.3	1.0111	1.3626	1.2270	3463	4.42
30	2.6	16.5	1.0122	1.3672	1.2262	3447	4.39
0	10.0	26.8	1.0126	1.3725	1.2262	3437	4.56
-90	-2.2	-5.4	1.0095	1.3588	1.2305	3483	4.85
-145	2.2	0.9	1.0085	1.3540	1.2333	3496	5.25
-165, -44 (α')	-4.1	18.2	1.0124	1.3701	1.2260	3443	4.71
-155, 159 (C5)	-3.2	-3.6	1.0106	1.3568	1.2321	3468	4.93
-134, 180	-1.9	-8.6	1.0104	1.3581	1.2320	3470	5.00
145	-4.0	-6.5	1.0107	1.3577	1.2319	3467	4.53
120	-2.2	-6.7	1.0106	1.3582	1.2315	3469	4.13
90	0.2	-8.3	1.0115	1.3605	1.2299	3457	3.62
60	-1.5	-6.1	1.0112	1.3606	1.2288	3463	3.43
30	-1.6	6.6	1.0108	1.3598	1.2290	3467	3.63
0	3.9	17.8	1.0119	1.3627	1.2285	3448	3.98
-90	-4.7	-14.2	1.0087	1.3670	1.2267	3471	5.31
-145	1.5	-4.2	1.0087	1.3578	1.2316	3493	5.31
-113, 13 (β_2)	0.1	10.7	1.0107	1.3584	1.2295	3468	3.40
-90, 180	-2.9	-14.6	1.0110	1.3631	1.2283	3460	4.70
145	-6.0	-14.6	1.0115	1.3606	1.2301	3456	3.89
120	-5.2	-16.7	1.0120	1.3602	1.2304	3453	3.23
90	-3.6	-18.1	1.0157	1.3604	1.2295	3404	2.40
60	1.5	2.8	1.0172	1.3558	1.2302	3369	2.11
30	5.3	22.0	1.0143	1.3603	1.2290	3420	2.31
0	1.3	13.5	1.0101	1.3570	1.2296	3476	3.06
-50	7.1	23.3	1.0124	1.3682	1.2255	3441	4.11
-90	-5.4	-14.0	1.0100	1.3691	1.2253	3473	5.26
-145	0.4	-6.6	1.0086	1.3627	1.2279	3493	5.27
-83, 75 (C7eq)	-2.2	-12.1	1.0178	1.3568	1.2304	3363	2.09
-60, 180	-3.7	-18.4	1.0116	1.3659	1.2258	3451	4.48
145	-7.2	-21.0	1.0118	1.3625	1.2279	3451	3.54
120	-8.1	-25.3	1.0127	1.3610	1.2294	3445	2.81
90	-8.0	-24.7	1.0167	1.3581	1.2311	3387	2.11
60	-2.2	-4.9	1.0191	1.3509	1.2326	3325	1.87
30	6.0	19.8	1.0190	1.3539	1.2317	3325	1.87
0	10.1	28.5	1.0126	1.3596	1.2299	3444	2.16
-40 (α_R)	4.6	21.6	1.0119	1.3624	1.2260	3449	2.68
-90	0.2	6.0	1.0095	1.3683	1.2234	3477	4.84
-145	-0.6	-11.1	1.0089	1.3661	1.2255	3489	5.16
-30, 180	-5.7	-22.5	1.0125	1.3718	1.2235	3439	4.65
145	-7.8	-23.4	1.0120	1.3655	1.2260	3447	3.67
120	-6.8	-27.2	1.0120	1.3627	1.2273	3449	3.03
90	-9.6	-31.2	1.0141	1.3598	1.2298	3425	2.26
60	-9.3	-21.1	1.0207	1.3514	1.2327	3300	1.84
30	-1.1	2.7	1.0225	1.3442	1.2345	3248	1.75
0	9.0	22.5	1.0211	1.3496	1.2330	3283	1.79
-30	13.6	32.2	1.0132	1.3616	1.2290	3433	2.10
-60	4.9	28.2	1.0126	1.3673	1.2246	3437	2.91
-90	5.2	25.7	1.0123	1.3689	1.2237	3442	3.61
-145	1.5	-6.7	1.0080	1.3694	1.2218	3499	5.31
0, 180	-6.7	-23.7	1.0123	1.3795	1.2185	3438	5.13
90	-3.5	-29.8	1.0125	1.3662	1.2244	3440	2.93
60	-12.9	-34.8	1.0145	1.3634	1.2274	3416	2.11
20	-8.0	-14.8	1.0243	1.3445	1.2343	3221	1.74
0	-0.5	0.7	1.0247	1.3410	1.2355	3210	1.72
-30	10.5	22.3	1.0230	1.3485	1.2337	3255	1.78
-50	15.0	32.4	1.0191	1.3584	1.2310	3338	1.92
-90	5.1	30.7	1.0121	1.3658	1.2259	3445	2.90
30, 30	-15.1	-32.9	1.0143	1.3622	1.2286	3415	2.03
0	-9.3	-20.5	1.0216	1.3485	1.2334	3274	1.78
-30	1.3	0.1	1.0224	1.3435	1.2353	3255	1.76
-60	10.2	22.4	1.0205	1.3518	1.2338	3305	1.85
-90	11.2	31.9	1.0138	1.3602	1.2308	3430	2.25

least two causes, the increasing electrical force that elongates the bond and the intrinsic contribution from the cross-term force constant $f(\text{NH s}, \text{NH ib})$ which, being negative, also leads to an elongating force on the NH bond as the NH ib angle

increases. These results emphasize the many factors that determine the $r-\gamma$ and $r-\nu$ relationships in peptide systems.

Another feature of the "hydrogen-bonded" structures is seen in the values of $\partial\mu/\partial r(\text{NH1})$. In Figure 11 we show the values

TABLE 6: (Continued)

φ, ψ^a	ω^b	γ^c	$r(\text{NH})^d$	$r(\text{CN})^d$	$r(\text{CO})^d$	$\nu(\text{NH})^e$	$\text{H}_{11}\cdots\text{O}_8^d$
61, 145	0.3	14.2	1.0115	1.3695	1.2239	3452	5.21
120	0.9	9.9	1.0103	1.3700	1.2235	3467	5.29
90	-2.0	-14.3	1.0109	1.3714	1.2217	3458	4.69
60	-5.0	-24.3	1.0128	1.3696	1.2228	3437	3.62
30	-4.0	-19.3	1.0103	1.3608	1.2270	3472	2.90
0	-11.7	-28.7	1.0143	1.3592	1.2301	3419	2.10
-30	-5.6	-17.3	1.0190	1.3523	1.2326	3325	1.88
-60	3.3	7.5	1.0189	1.3510	1.2336	3329	1.89
-90	9.0	25.8	1.0161	1.3586	1.2316	3397	2.14
-120	6.6	23.4	1.0112	1.3586	1.2300	3463	2.92
73, 17 (α_1)	-3.9	-16.6	1.0098	1.3580	1.2287	3480	2.86
73, -55 (C7ax)	0.5	0.2	1.0186	1.3520	1.2327	3337	1.94

^a Torsion angles: $\varphi = \tau(\text{C}_2\text{N}_3\text{C}_4\text{C}_5)$, $\psi = \tau(\text{N}_3\text{C}_4\text{C}_5\text{N}_6)$, in degrees. ^b Peptide group (Bell's) torsion angle, in degrees. ^c NH out-of-plane bend angle, in degrees. The sign of γ is defined as follows: referring to Figure 1, in the planar sequence $\text{C}_5\text{-N}_6\text{H}_{11}\text{-C}_7$, positive γ corresponds to the displacement of H in the direction of a right-handed screw advancing with a rotation of $\text{H}_{11}\text{-C}_7\text{-C}_5$. ^d In angstroms. ^e In cm^{-1} .

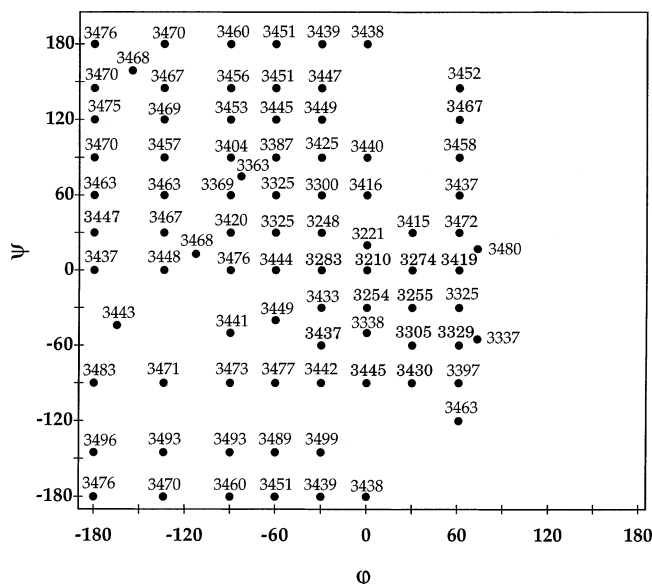


Figure 7. NH2 stretch vibrational frequency map (in cm^{-1}) of conformers of the alanine dipeptide as a function of $\varphi(\text{CNC}^i\text{C})$ and $\psi(\text{NC}^i\text{CN})$ (in degrees).

of this dipole derivative as a function of $r(\text{NH})$ for some of the conformers. It is clear that the values fall in two groups: those in which $\partial\mu/\partial r(\text{NH1})$ decreases essentially linearly with r ; and another set which show a generally increasing $\partial\mu/\partial r(\text{NH1})$ with r . In the first set are structures for which $r(\text{H}_9\cdots\text{O}_{10}) > 3 \text{ \AA}$, and thus any interaction between peptide group 2 and NH1 is minimal. This represents the behavior of the *intrinsic* dipole derivative and is seen to be similar to that in NMA, with similar values and (if more pronounced) negative slope. In the second set are structures for which $r(\text{H}_9\cdots\text{O}_{10}) < 3 \text{ \AA}$, corresponding to some of the “hydrogen-bonded” structures: $r(\text{H}_9\cdots\text{O}_{10}) = 2.61, 2.17, 2.17, \text{ and } 2.09 \text{ \AA}$ for points at $r(\text{NH1}) = 1.0127$ ($-134, 120$), 1.0145 ($-180, -145$), 1.0159 ($-134, 180$), and 1.0154 ($-180, 180$) \AA , respectively. In these cases the enhanced electrical interaction with peptide group 2 and the consequent increase in the *induced* $\partial\mu/\partial r$ (which is determined by the NH1 polarizability derivative as well as the external electric field due to group 2) with smaller $r(\text{H}_9\cdots\text{O}_{10})$,⁶ which adds to the parallel *intrinsic* $\partial\mu/\partial r$, leads to a total $\partial\mu/\partial r$ whose behavior is increasingly dominated by the *induced* $\partial\mu/\partial r$. We will see this effect demonstrated much more dramatically for $\partial\mu/\partial r(\text{NH2})$.

Our use of the terms “red-shifted” and “blue-shifted” frequencies implies that it is meaningful and possible to identify unperturbed NH1 s modes and therefore to infer the nature of physical factors that produce shifts from these frequencies. With

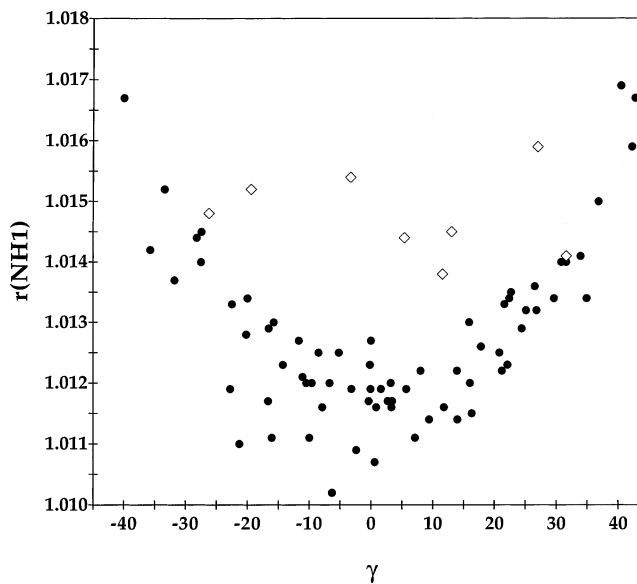


Figure 8. NH1 bond length (in angstroms) of conformers of the alanine dipeptide, as a function of the nitrogen pyramidalization angle γ (in degrees).

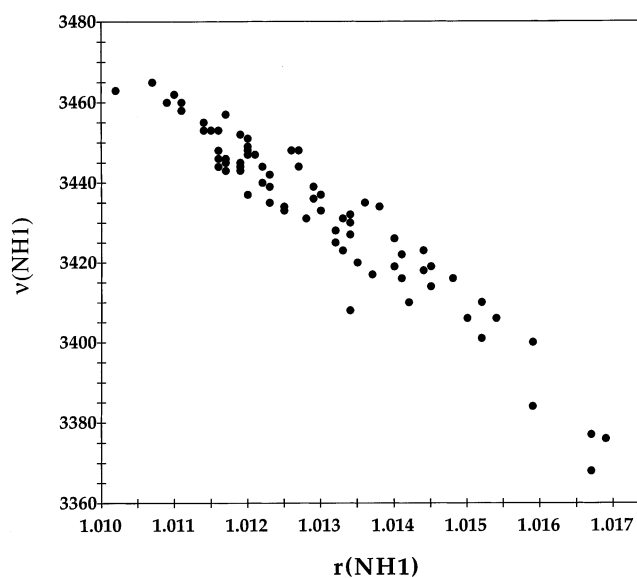


Figure 9. NH1 stretch frequency (in cm^{-1}) of conformers of the alanine dipeptide as a function of the NH1 bond length (in angstroms).

NMA as a guide, we should be justified in this respect in selecting conformations in which ω and γ are close to zero, no strong HB to the group is involved, and the NH1 ib and NH2

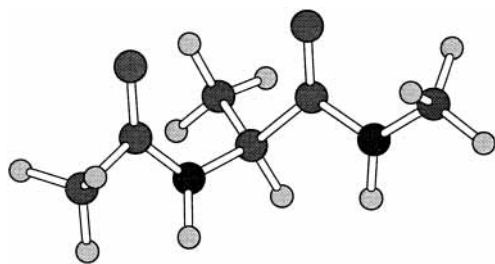


Figure 10. Alanine dipeptide in the $\varphi = 61^\circ$, $\psi = 90^\circ$ conformation.

s contributions to the NH1 s eigenvector (the NH1 s coordinate contribution taken as 1.000) are small, as are other coordinate contributions. No single conformer satisfies all of these criteria, but some are close; giving ω , γ , NH ib, NH2 s, and ν , we find for 0,60: $-3.8, 5.7, 0.000, -0.025, 3443$; $-134,120: 0.6, 0, -0.018, 0.027, 3448$; $-90,90: 4.2, 2.7, -0.003, -0.010, 3457$. These results suggest that frequencies in the range of $3450 \pm 10 \text{ cm}^{-1}$ probably represent minimally perturbed NH1 s modes, and thus give some quantitative basis for designating our maximally red-shifted (82 cm^{-1}) and blue-shifted (13 cm^{-1}) frequencies.

Returning to the spread in the r - γ (Figure 8) and ν - r (Figure 9) relations, there is one other important contributing factor in addition to the influence of nonbonded and electric field-induced effects, viz., conformationally sensitive variations in the NH s eigenvector. In comparing contributions to this eigenvector of other coordinates in the ADP as a function of φ and ψ , we find the following:

(1) CN s, NC^α s, C(Me)CN deformation (d), CNC^α d, and CO ib show only small variations, as in NMA (Table 2).

(2) The magnitude of NH ib is quite variable, from 0 to 0.048, with no clear dependence on γ .

(3) NH ob, CN t, and NC^α t again show the linear dependence on γ .

(4) New coordinates in the ADP show large regular variations with φ and ψ , with no clear dependence on γ : thus NC^α C d varies between 0.003 and 0.034, H^α bend1 (b1) varies between 0.002 and 0.020, H^α b2 varies between 0.002 and 0.033, C^β b1 varies between 0.000 and 0.048, and C^β b2 varies between 0.001 and 0.032. The complex combination of these various influences on $r(\text{NH})$ and $\nu(\text{NH})$ undoubtedly superimposes on the simple features in NMA, represented in Figures 2 and 3, to produce the bands of values in the ADP, as seen in Figures 8 and 9.

An important result of the analysis of the NH1 s normal mode of the ADP conformers is that this frequency, even in the absence of standard hydrogen bonding, can vary over a range of almost 100 cm^{-1} . While this may be counterintuitive for a "localized vibration", the reality is that such modes are not totally isolated from the internal structural environment, and caution is needed in assigning simple causes to observed frequency shifts. An important consequence, which should not be surprising in view of our previous discussion, is that a particular value of $\nu(\text{NH})$ does not necessarily correlate with a specific $r(\text{NH})$ or with a peptide group structure. A good example of this is given by the four structures at $-134,120$, $-90,120$, $-90,30$, and $30,30$, all of which have $\nu(\text{NH}) = 3448 \text{ cm}^{-1}$ but varying $r(\text{NH1})$ (1.0127, 1.0126, 1.0120, and 1.0116 Å) and other peptide geometry parameters.

3.2.3. Peptide Group 2. In contrast to NH1 s, the frequency range for NH2 s is much larger, from 3210 cm^{-1} (for 0,0) to 3499 cm^{-1} (for 30,-145). The significant extension to lower frequencies is a consequence of the formation of traditional HBs, as usually exemplified by the C7eq and C7ax structures.²⁴

However, it is important to note that these two structures, although at energy minima²⁵ (Figures 5 and 7), do not form the strongest HBs, having NH s frequencies of 3363 (C7eq) and 3337 (C7ax) cm^{-1} : a group of higher energy structures centered around a diagonal from $-30,30$ to $30,-30$ (Figure 7), all have frequencies below 3300 cm^{-1} . Of course, HB strength (i.e., favorable energy) is only one component of the total energy, and it is important to keep this in mind in evaluating spectroscopic results.

In the case of NH1, it seemed possible to identify a frequency region of relatively "unperturbed" NH s frequencies. Is the same possible for NH2 s modes, thus enabling some physical insights into the sources of frequency shifts from this region? Again using NMA as a guide (except that its unperturbed frequency of 3500 cm^{-1} does not reflect the possible influence of the CH_3 side chain in the ADP), we should target conformations in which ω and γ are close to zero, no HB type of interaction to the group is involved, and the NH2 ib and NH1 s contributions to the NH2 s eigenvector are small. In addition, since the (N)CH₃ rock2 (r_2)²³ contribution in NMA varies significantly with γ (Table 2), we should require this contribution to be small. Several conformers fall in this range; giving ω , γ , NH2 ib, NH1 s, (N)CH₃ r_2 , and ν , we find for $-180,90: 0.4, -3.5, 0.005, -0.003, -0.008, 3470$; $-180,60: -0.4, 1.3, 0.010, -0.002, 0.003, 3463$; $-180,-90: -2.2, -5.4, 0.004, -0.004, -0.010, 3483$. This suggests that frequencies in the range of $3473 \pm 10 \text{ cm}^{-1}$ probably represent "minimally perturbed" NH2 s modes, indicating that frequencies at the high end, that is, $\geq 3490 \text{ cm}^{-1}$, are blue-shifted. Although it may seem contradictory, we actually find structures that satisfy the above "unperturbed" criteria and yet have blue-shifted frequencies, $-180,-145: 2.2, 0.9, 0.004, -0.007, 0.003, 3496$; and $-90,-145: 0.4, -6.6, 0.000, 0.001, -0.010, 3493$. However, the cause of the shortened $r(\text{NH})$, and therefore high $\nu(\text{NH})$, of these structures is revealed by an examination of the environment of NH2: the distance between H_{11} and one of the (C^β) H^β atoms is very short, 2.07 \AA in the first case and 2.09 \AA in the second, and steric repulsion undoubtedly leads to some bond contraction.^{8,9} In fact, all of the $\psi = -145^\circ$ conformations have such a close contact, and it can be seen from Table 6 that all such conformers have the highest $\nu(\text{NH})$.

Examining relationships similar to those for NH1, we find the following.

(1) A plot of $r(\text{NH2})$ versus γ exhibits two behavior classes: for conformers with $\text{H}_{11}\cdots\text{O}_8 > 2.5 \text{ \AA}$, the plot is similar to that of Figure 8 but with a slightly smaller spread; for $\text{H}_{11}\cdots\text{O}_8 < 2.5 \text{ \AA}$, the points show no obvious pattern, although for this distance $< 2.00 \text{ \AA}$, all of the points, from $\gamma = -20^\circ$ to $> 30^\circ$, fall above $r(\text{NH}) = 1.0180 \text{ \AA}$.

(2) A plot of $\nu(\text{NH})$ versus $r(\text{NH})$, Figure 12, exhibits two regions of different slopes. This seems to be associated with the increasing contribution of NH ib to the NH s eigenvector: for structures in the $r(\text{NH}) = 1.0075$ to $r(\text{NH}) \sim 1.0160 \text{ \AA}$ region, the NH ib eigenvector contribution is generally and variably < 0.020 ; for structures with longer $r(\text{NH})$, corresponding to the formation of stronger HBs, this contribution steadily increases to 0.050 as $\text{H}_{11}\cdots\text{O}_8$ decreases. As in the case of peptide group 1 (see Table 7), this increase follows an increase in $f(\text{NH s}, \text{NH ib})$, from 0.014 (for $-180,-145$) to 0.146 (for 0,0). Also, as in the case of peptide group 1, this is due to the increasing local asymmetry associated with the HB environment of the NH group. The positive sign of this force constant, as contrasted with its negative sign in peptide group 1 (Table 7), is consistent with its positive sign and magnitude, 0.007, in the

TABLE 7: Peptide Group 1 Characteristics of Some $\varphi = -180^\circ$ Conformers of the Alanine Dipeptide

ψ^a	$r(\text{H}_9 \cdots \text{O}_{10})^b$	NH ib ^c	γ^a	$r(\text{NH})^b$	EV(NH ib) ^d	$f(\text{NH s, NH ib})^e$	$\nu(\text{NH})^f$
60	5.31	0.3	-27.5	1.0140	0.000	0.002	3419
90	2.85	1.0	-28.2	1.0144	-0.004	-0.013	3418
120	2.45	3.3	-26.2	1.0148	-0.017	-0.058	3416
145	2.24	5.3	-19.4	1.0152	-0.032	-0.109	3410
180	2.09	6.7	-3.3	1.0154	-0.047	-0.153	3406

^a In degrees. ^b In angstroms. ^c NH ib = $\text{C}_2\text{N}_3\text{H}_9 - \text{C}_4\text{N}_3\text{H}_9$, in degrees. ^d Contribution to NH stretch eigenvector; NH s coordinate taken as 1.000. ^e Interaction force constant between NH stretch and NH in-plane bend, in mdyn. ^f Frequency in cm^{-1} .

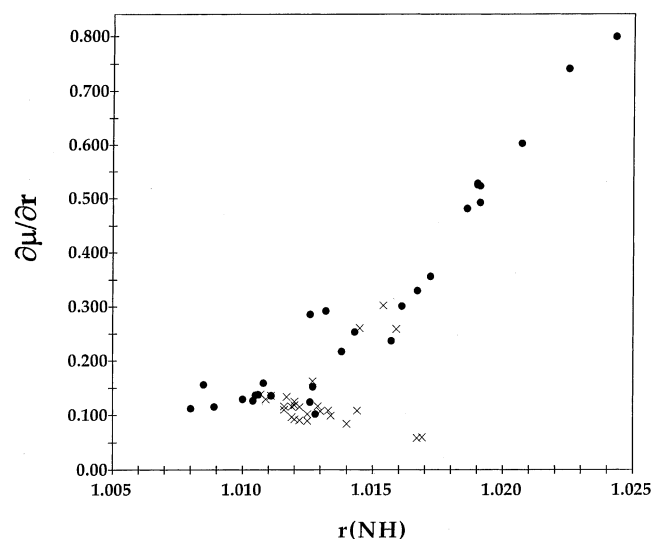


Figure 11. Dipole derivative (in electrons) of NH1 (x) and NH2 (●) of some conformers of the alanine dipeptide as a function of the NH bond length (in angstroms).

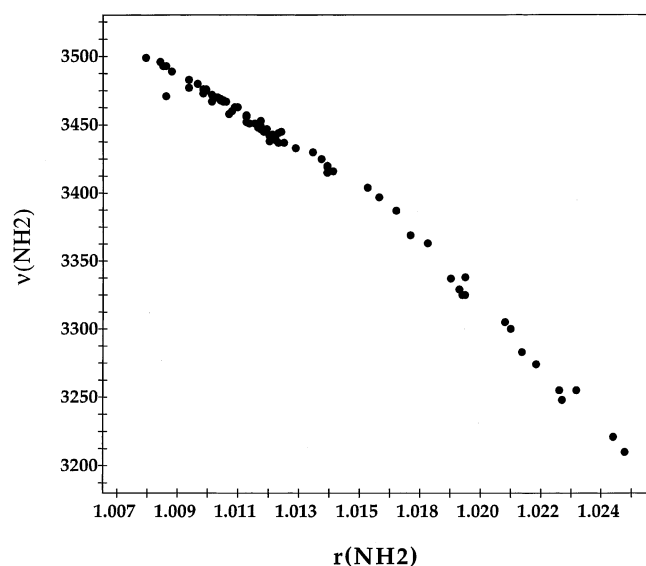


Figure 12. NH2 stretch frequency (in cm^{-1}) of conformers of the alanine dipeptide as a function of the NH2 bond length (in angstroms).

similar surroundings of NMA (in which, however, the environment is more symmetric). We note, however, that the value of $f(\text{NH s, NH ib})$ is not always a dominating factor in determining $\nu(\text{NH})$: although these values are similar for NH1 at $-180, -180$ (-0.153) and NH2 at $0, 0$ (0.146), the bond lengths (and frequencies) are quite different, 1.0154 (3406 cm^{-1}) and 1.0247 \AA (3210 cm^{-1}), respectively. This may be due (in addition to the different chemical environments) to the much larger elongating force on NH2 from the closer dipolar electric field of group 1 in the latter case than in the former.^{6,9} (Note that the large bond elongation in the second case occurs despite the large

contracting force due to the repulsive interaction associated with the short $\text{H} \cdots \text{O}$ distance, 1.72 \AA , at least as compared to those of the low-energy equilibrium structures C7eq (2.09 \AA) and C7ax (1.94 \AA).

(3) The NH ob contribution to the NH s eigenvector is still proportional to $|\gamma|$, as for NH1 (Figure 4), but its effect on $r(\text{NH})$ can be overwhelmed by other factors, such as hydrogen bonding: compare, both at $\gamma = 22^\circ$, $r(\text{NH2}) = 1.0143 \text{ \AA}$ for $-90, 30$ and $r(\text{NH2}) = 1.0230 \text{ \AA}$ for $0, -30$. In fact, in the group of non-hydrogen-bonded structures represented in the left-hand part of Figure 12, the trend to longer $r(\text{NH})$ roughly follows increases in $|\gamma|$.

(4) Even for typical hydrogen-bonded groups, constancy of $\nu(\text{NH})$ does not imply constancy of $r(\text{NH})$ or peptide structure and therefore constancy of HB strength. Good examples of this are the pairs of structures $0, -30$ and $30, -30$ as well as $0, -50$ and $73, -55$.

(5) The $\partial\mu/\partial r(\text{NH2})$, Figure 11, again fall into two groups: those in which $\partial\mu/\partial r$ decreases essentially linearly with $r(\text{NH})$, representing the *intrinsic* $\partial\mu/\partial r$, in fact falling in the same curve as that for $\partial\mu/\partial r(\text{NH1})$ (the $r(\text{NH2}) = 1.0080 \text{ \AA}$ point for $-30, -145$, corresponds to a maximally blue-shifted mode arising from a contracting electric field–dipole derivative interaction⁶); and those corresponding to the formation of increasingly strong standard hydrogen bonds. As noted in connection with NH1, such interactions lead to a dominance of the *induced* dipole derivative, which is always associated with a positive second dipole derivative,⁶ and thus the total $\partial\mu/\partial r$ of these NH bonds increases at a huge rate as $r(\text{NH2})$ increases (with smaller $r(\text{H}_{11} \cdots \text{O}_8)$). Since the intensity of an infrared band is proportional to the square of $\partial\mu/\partial r$, it is understandable how hydrogen bonding leads to large increases in the intensity of $\nu(\text{XH})$ bands.

4. Conclusions

The structural and vibrational analyses of *N*-methylacetamide and 78 conformers of the alanine dipeptide have provided deeper insights into the many physical factors that determine the spectroscopic shifts in the frequencies of their NH stretch modes. Despite claims to the contrary,¹⁶ examination of Jacobian elements show that these conclusions are not affected by the constraints imposed on the φ and ψ torsion angles of the ADP structures in these studies.

The up to $\sim 300 \text{ cm}^{-1}$ red-shifts of $\nu(\text{NH2})$ of the ADP that can result from the participation of this group in the standard type of hydrogen bond are not surprising (although it may be surprising to realize that shifts of only about half of this magnitude are associated with the HBs of the “typical” C7eq and C7ax equilibrium structures). However, the $\sim 100 \text{ cm}^{-1}$ variation in $\nu(\text{NH1})$, which is not involved in standard hydrogen bonding, as a function of φ and ψ highlights the influence of other environmental factors in determining $r(\text{NH})$ and therefore (partially) $\nu(\text{NH})$. Our studies indicate that the most important factors affecting NH s frequencies (and indeed intensities) are the following:

(1) *Pyramidalization of the nitrogen atom.* We had shown previously¹⁰ that departures from peptide group planarity (nonzero ω) lead to equilibrium pyramidalization of the nitrogen (nonzero γ). We now find, in studies of NMA as well as the ADP, that any pyramidalization of the nitrogen, whether caused by peptide nonplanarity or steric interactions, will result in elongation of the NH bond. This is undoubtedly a result of the reorganization of the electronic structure of the peptide group. A relevant consequence of such increasing pyramidalization is a proportional increase in the NH ob component of the eigenvector associated with the NH s mode.

(2) *Electrical and steric effects.* Our previous studies^{6,9} had shown that $r(\text{NH})$ will be influenced by forces that arise from external electric fields and repulsive interactions: the former always leads to bond elongation if field and NH dipole derivative are parallel and usually to bond contraction if these are antiparallel; the latter always leads to bond contraction. Both of these effects are evident in frequency shifts found in the ADP structures and are obviously a function of conformation.

(3) *Hydrogen bonding.* Although we conceptually describe the formation of a HB as a separate environmental factor, in fact it is really only a stronger manifestation of the electric field plus repulsion effects⁹ (this does not exclude the occurrence of accompanying phenomena, such as charge transfer and other electronic structural changes, that result from the eventual overlap of the wave functions of donor and acceptor molecules).

(4) *Intrinsic force field effects.* The existence of interaction force constants between NH s and other coordinates results in forces on the NH bond when these coordinates are deformed as a consequence of conformational changes. This effect may not be negligible.⁹

(5) *Eigenvector change.* Although NH s is a highly localized mode, it is not completely so, and other internal coordinates contribute to a degree that can vary with conformation. As we find in the ADP, the rate of variation of $\nu(\text{NH})$ with $r(\text{NH})$ can depend on which coordinates contribute significantly in particular circumstances, such as the increasing contribution of NH ib to the NH s eigenvector with increasing HB strength.

(6) *Dipole derivative changes.* We find that the increase in intensity of the NH s infrared band with increasing HB strength is completely consistent with an electric field-based description of this interaction, viz., the increasing dominance of the NH induced dipole derivative as $r(\text{H}\cdots\text{O})$ decreases, in determining the total value of $\partial\mu/\partial r(\text{NH})$. This emphasizes the primary and comprehensive character of the electrical origin in describing the nature of hydrogen bonding.

In observing that $\nu(\text{NH}_2)$ of the lowest energy hydrogen-bonded ADP structure, C7eq, viz., 3363 cm^{-1} , is almost the same as $\nu(\text{NH}_1)$ of other non-hydrogen-bonded (high energy) structures, for example, 3377 cm^{-1} of $-180,0$, it should be clear that, even allowing for the different chemical nature of these groups, caution is needed in simply relating shifts in $\nu(\text{NH})$ to the strengths of hydrogen bonding. (Of course, local high-energy conformations would have to be compensated by conformations in other parts of the structure that result in an overall minimum energy.) Each potentially hydrogen-bonded system is different, and the main message may be that in the vibrational analyses

each amide or peptide system should be carefully studied to determine all the likely contributors to shifts in the NH stretch frequency.

Acknowledgment. This research was supported by NSF Grants DMR-0239417 and MCB-0212232. We are grateful for support by NSF cooperative agreement ACI-9619029 through computing resources provided by the National Partnership for Advanced Computational Infrastructure at the San Diego Supercomputer Center. We appreciate helpful discussions with Weili Qian and Kim Palmo.

Supporting Information Available: Relative energies of alanine dipeptide conformers. This material is available free of charge via the Internet at <http://pubs.acs.org>.

References and Notes

- (1) Pimentel, G. C.; McClellan, A. L. *The Hydrogen Bond*; W. H. Freeman and Co.: San Francisco, 1960.
- (2) van Duijneveldt-van de Rijdt, J. G. C. M.; van Duijneveldt, F. B.; Kanters, J. A.; Williams, D. R. *J. Mol. Struct. (THEOCHEM)* **1984**, *109*, 351–366.
- (3) Cheam, T. C.; Krimm, S. *J. Mol. Struct.* **1986**, *146*, 175–189.
- (4) Liu, S.; Dykstra, C. E. *J. Phys. Chem.* **1986**, *90*, 3097–3103.
- (5) Hermansson, K. *J. Phys. Chem. A* **2002**, *106*, 4695–4702.
- (6) Qian, W.; Krimm, S. *J. Phys. Chem. A* **2002**, *106*, 6628–6636.
- (7) Dinur, U. *Chem. Phys. Lett.* **1992**, *192*, 399–406.
- (8) Li, X.; Liu, L.; Schlegel, H. B. *J. Am. Chem. Soc.* **2002**, *124*, 9639–9647.
- (9) Qian, W.; Krimm, S. *J. Phys. Chem. A* **2002**, *106*, 11663–11671.
- (10) Mannfors, B. E.; Mirkin, N. G.; Palmo, K.; Krimm, S. *J. Phys. Chem. A* **2003**, *107*, 1825–1832.
- (11) Palmo, K.; Mannfors, B.; Mirkin, N. G.; Krimm, S. *Biopolymers* **2003**, *68*, 383–394.
- (12) Mirkin, N. G.; Krimm, S. *J. Phys. Chem. A* **2002**, *106*, 3391–3394.
- (13) Frisch, M. J.; Trucks, G. W.; Schlegel, H. B.; Scuseria, G. E.; Robb, M. A.; Cheeseman, J. R.; Zakrzewski, V. G.; Montgomery, J. A., Jr.; Stratmann, R. E.; Burant, J. C.; Dapprich, S.; Millam, J. M.; Daniels, A. D.; Kudin, K. N.; Strain, M. C.; Farkas, O.; Tomasi, J.; Barone, V.; Cossi, M.; Cammi, R.; Mennucci, B.; Pomelli, C.; Adamo, C.; Clifford, S.; Ochterski, J.; Petersson, G. A.; Ayala, P. Y.; Cui, Q.; Morokuma, K.; Malick, D. K.; Rabuck, A. D.; Raghavachari, K.; Foresman, J. B.; Cioslowski, J.; Ortiz, J. V.; Stefanov, B. B.; Liu, G.; Liashenko, A.; Piskorz, P.; Komaromi, I.; Gomperts, R.; Martin, R. L.; Fox, D. J.; Keith, T.; Al-Laham, M. A.; Peng, C. Y.; Nanayakkara, A.; Gonzalez, C.; Challacombe, M.; Gill, P. M. W.; Johnson, B. G.; Chen, W.; Wong, M. W.; Andres, J. L.; Head-Gordon, M.; Replogle, E. S.; Pople, J. A. *Gaussian 98*, revision A.9; Gaussian, Inc.: Pittsburgh, PA, 1998.
- (14) Mirkin, N. G.; Krimm, S. *J. Mol. Struct. (THEOCHEM)* **1995**, *334*, 1–6.
- (15) Bell, B. P. *Trans. Faraday Soc.* **1945**, *41*, 293–295.
- (16) Schweitzer-Stenner, R.; Eker, F.; Huang, Q.; Griebenow, K.; Mroz, P. A.; Kazlowski, P. M. *J. Phys. Chem. B* **2002**, *106*, 4294–4304.
- (17) Greenie, Y.; Avignon, M.; Garrigou-Lagrange, C. *J. Mol. Struct.* **1975**, *24*, 293–307.
- (18) Mirkin, N. G.; Krimm, S. To be submitted for publication.
- (19) Breneman, C. M.; Wiberg, K. B. *J. Comput. Chem.* **1990**, *11*, 361–373.
- (20) Krimm, S.; Abe, Y. *Proc. Natl. Acad. Sci. U.S.A.* **1972**, *69*, 2788–2792.
- (21) Moore, W. H.; Krimm, S. *Proc. Natl. Acad. Sci. U.S.A.* **1975**, *72*, 4933–4935.
- (22) Cheam, T. C.; Krimm, S. *Chem. Phys. Lett.* **1984**, *107*, 613–616.
- (23) Mirkin, N. G.; Krimm, S. *J. Mol. Struct.* **1991**, *242*, 143–160.
- (24) Cheam, T. C.; Krimm, S. *J. Mol. Struct. (THEOCHEM)* **1989**, *188*, 15–43.
- (25) Scardsdale, J. N.; Van Alsenoy, C.; Klimkowski, V. J.; Schäfer, L.; Momany, F. A. *J. Am. Chem. Soc.* **1983**, *105*, 3438–3445.